

Document downloaded from:

<http://hdl.handle.net/10251/186860>

This paper must be cited as:

Arnau Martínez, FJ.; Martín, J.; Pla Moreno, B.; Auñón-García, Á. (2021). Diesel engine optimization and exhaust thermal management by means of variable valve train strategies. *International Journal of Engine Research*. 22(4):1196-1213.  
<https://doi.org/10.1177/1468087419894804>




The final publication is available at

<https://doi.org/10.1177/1468087419894804>

Copyright SAGE Publications

Additional Information

# Diesel Engine Optimization and Exhaust Thermal Management by Means of Variable Valve Train Strategies

Journal Title  
XX(X):1-17  
©The Author(s) 0000  
Reprints and permission:  
sagepub.co.uk/journalsPermissions.nav  
DOI: 10.1177/ToBeAssigned  
www.sagepub.com/  


Francisco J. Arnau<sup>1</sup>, Jaime Martín<sup>1</sup>, Benjamín Pla<sup>1</sup> and Ángel Auñón<sup>1</sup>

## Abstract

Due to the need to achieve a fast warm-up of the after-treatment system in order to fulfill the pollutant emission regulations, a growing interest has arisen to adopt Variable Valve Timing (VVT) technology for automotive engines. Several VVT strategies can be used to achieve an increment in the after-treatment upstream temperature by increasing the residual gas amount.

In this paper, a one-dimensional gas dynamics engine model has been used to carry out a simulation study comparing several exhaust variable valve actuation strategies. A steady-state analysis has been done in order to evaluate the potential of the different strategies at different operating points. Finally, the effect on the after-treatment warm-up, fuel economy and pollutant emission levels was evaluated over the WLTC (Worldwide harmonized Light vehicles Test Cycle). As a conclusion, the combination an advanced exhaust (EEVO and EEVC) and a delayed intake (LIVO and LIVC) presented the best trade-off between exhaust temperature increment and fuel consumption, which achieved a mean temperature increment during low speed phase of the WLTC of 27°C with a fuel penalty of 6%. The exhaust valve re-opening technique offers a worse trade-off. However, the exhaust valve re-opening leads to lower NO<sub>x</sub> (29% less) and CO (11% less) pollutant emissions.

## Keywords

Variable valve actuation, variable valve timing, light-duty diesel engine, aftertreatment thermal management, one-dimensional model, World Harmonized Light-duty Vehicle Test Procedure, light-off temperature, diesel engine emissions

## Introduction

One of the major goals of engine developers and manufacturers is to minimize fuel consumption and emissions. Specially in diesel engines, a great challenge is the cold start and heating phase, since heating techniques are a compromise between a fast heat-up of the after-treatment system and a low penalty in fuel consumption. In this context, the VVT of the exhaust valves can be a key technology for increasing after-treatment system temperatures after cold start and during warm up.

Concerning the fuel consumption improvements, VVT has traditionally been used widely in SI engines rather than in CI engines. At low loads, the pumping losses in gasoline engines are greater than those of diesel engines because of the intake throttling. Without a throttle valve, the control of the air-fuel mixture can be achieved by variation of the intake valve opening period; therefore, the VVT has great potential for reducing pumping losses in gasoline engines. In diesel engines, whose control of load is performed by regulating the amount of fuel injected, pumping losses at partial loads are lower. The application of VVT in diesel engines is restricted due to the small clearance height between piston and cylinder head at TDC, which allows reaching higher compression ratios than in gasoline engines. This restriction means that the valves can have a little or no lift at overlap TDC, which involves a reduced margin for advancing the intake opening and retarding the exhaust closing in order to avoid valve to piston contact. Contrarily, there are no restrictions

regarding the exhaust opening and intake closing events. As a consequence, conventional camshaft phasers are used very little in diesel engines, but systems that provide control over the valve open period, and or duration, can be applied<sup>1</sup>.

However, in order to optimize the cold start and the heating phase, VVT applications have shown a great potential in diesel engines, making it possible to provide the residual gas required for this situation<sup>2,3</sup>. This leads to a reduction of CO and HC emissions that are intrinsic to the cold start.

In this paper, a simulation study is presented comparing different exhaust valve actuation strategies in order to increase exhaust temperature of a light-duty diesel engine.

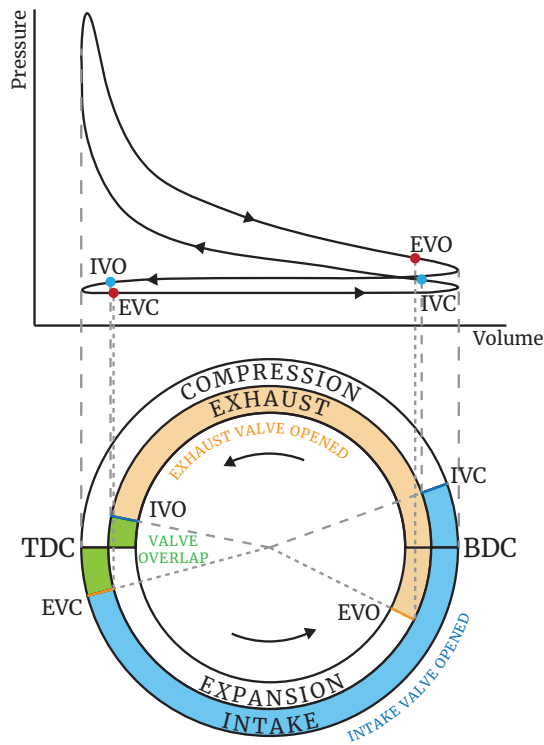
## Valve events of a four-stroke engine

Figure 1 shows the valve timing diagram of a conventional light-duty diesel engine. In that diagram one can differentiate four valve events: intake opening and closing (IVO and IVC), and exhaust opening and closing (EVO and EVC).

<sup>1</sup>CMT - Motores Térmicos, Universitat Politècnica de València, ES

## Corresponding author:

Francisco José Arnau Martínez, CMT - Motores Térmicos, Universitat Politècnica de València,  
Camino de Vera s/n, Valencia 46022, Spain  
Email: [farnau@mot.upv.es](mailto:farnau@mot.upv.es)



**Figure 1.** Four stroke diesel engine P-V diagram (top) and engine timing diagram (bottom).

### Variable valve timing strategies

The four different valve events described above are fixed in conventional cam actuation system. Thus, the timing of these valve events is the result of a performance compromise under different operating conditions. Variable valve timing strategies arise from the need to find the most efficient way to operate the engine depending on its engine speed and load at any point of the engine map. Consequently, different approaches can be described by advancing or delaying the different valve events:

**Early Intake Valve Opening (EIVO).** By advancing the IVO event, intake valve opens before TDC during the exhaust stroke. Thus, increasing the valve overlap and the amount of burnt gases backflow into the intake ports. This part of exhaust gases mixes with fresh air from the intake manifold and serves as an internal gas recirculation (IGR), reducing the combustion temperature and, consequently, reducing the  $\text{NO}_x$  amount<sup>4</sup> produced during the combustion. Experiments carried on by Tomoda et al.<sup>5</sup>, in a 2.2 litres Diesel engine, found that advancing the IVO timing before TDC results in an improvement of the swirl ratio and an increase in the introduced air mass at low and high load. This effect leads to a better trade-off between  $\text{NO}_x$  and fuel consumption. The fuel economy improvement is produced by and enhanced combustion rate due to the higher swirl ratio and the reduction in pumping losses due to de early IVO<sup>5</sup>.

**Late Intake Valve Opening (LIVO).** The duration of the valve overlap depends on several factors: the distance between piston and cylinder head at TDC (which usually is lower in a diesel engine due to the high compression ratio), the engine speed and the instantaneous pressures at

intake and exhaust ports. In diesel engines, when pressure is higher in exhaust manifold, valve overlap should be reduced to avoid backflows into intake manifold<sup>6</sup>. Delaying the IVO event reduces valve overlap, leading to a very low or insignificant backflow into intake manifold. Deppenkemper et al.<sup>7</sup> found, using a one-dimensional engine model, that if the IVO is delayed up to the beginning of the intake stroke, the velocity at which the air enters into the cylinder will be higher due to the lower pressure inside the cylinder. This increase in inlet air velocity enhances in-cylinder turbulence, which improves the mixing process, resulting in lower HC emissions.

**Early Intake Valve Closing (EIVC).** Backflow during the compression stroke can be reduced or avoided by advancing IVC. EIVC strategy reduces the amount of air admitted into the cylinder and thereby reduces slightly the work required for filling the cylinder when compared with a conventional valve timing. Zammit et al.<sup>8</sup> found that EIVC decreases  $\text{NO}_x$  emissions for advances greater than  $30^\circ$  at low engine speeds and low loads, reduces soot levels and raises exhaust gas temperatures. Nevertheless, CO and HC engine-out emissions increases and fuel economy is deteriorated, since more fuel amount is required for a lower air charge<sup>8</sup>. Tomoda et al.<sup>5</sup> also claim that when the IVC timing is advanced towards BDC, the effective compression ratio increases and this creates an increased compression end temperature, so that HC formation is reduced. The increase in effective compression ratio also allows an increase of EGR rate, resulting in reduced  $\text{NO}_x$  emissions. At high loads, however, EIVC decreases the amount of charged air mass in the cylinder and results in an increase of HC emissions. According to Tomoda et al.<sup>5</sup>, early IVC on one intake valve relative to the other valve allows controlling the swirl strength, resulting in A  $\text{NO}_x$  and soot emissions reduction at high load because it reduces both pumping losses and fuel consumption.

**Late Intake Valve Closing (LIVC).** Performing a late intake valve means that intake valves are opened during the first part of the compression stroke. Consequently, some of the air flows back into the intake manifold, leading to a reduction in the effective compression ratio and a lambda reduction (lower combustion chamber charge). These two consequences lead to a higher exhaust gas temperatures and a  $\text{NO}_x$  engine-out emission reduction<sup>9-11</sup>. However, Maniatis et al.<sup>12</sup> experiments did not found any benefit in exhaust gas enthalpy nor a reduction of HC and CO emissions. Kim et al.<sup>13</sup> found that the amount of EGR could be reduced to maintain a similar level of  $\text{NO}_x$  emissions when the IVC timing is retarded. This characteristic also prevents an increase in soot emissions. The combination of EGR and LIVC helped to improve the  $\text{NO}_x$ -soot trade-off relation<sup>10,11</sup>. Similarly, Zhou et al.<sup>14</sup> achieved a reduction in particle matter emissions by 32.9% with a small increase in  $\text{NO}_x$  by applying LIVC strategy and an optimal control of the VGT and EGR during realistic transient conditions.

**Early Exhaust Valve Opening (EEVO).** The early opening of the exhaust valve provides better scavenging of the exhaust gases, but it also causes a reduction in the expansion work, resulting in a reduction of the engine brake power, thus worsening the fuel consumption. EEVO also produces

an increment in exhaust pressure and temperature levels higher than those obtained with the standard valve timing. The greater the advance in EVO, the larger increment in exhaust temperature, but with a larger penalty in terms of BSFC<sup>9,15</sup>. Regarding pollutant emissions, EEVO results in an increase in engine-out hydrocarbons and CO because their oxidation during the expansion stroke is interrupted with the early EVO<sup>4,16</sup>. In studies carried on by Gossala et al.<sup>15</sup> at idle conditions, the fuel penalty caused by early EVO produces more NO<sub>x</sub> and particle matter emissions due to the higher injected fuel mass. Particle matter emissions can be reduced by increasing the air-fuel ratio, but it also reduces the exhaust temperature increment.

*Late Exhaust Valve Opening (LEVO).* When performing LEVO, the exhaust valve is opened later than usual, near BDC or after this point. In this case, a greater expansion work is produced without losses during the power stroke. However, exhaust pumping work increases because of a very late EVO, which results in some restriction to expel the exhaust gases out of the cylinder. According to Piano<sup>9</sup>, a fast opening lift of the exhaust valve is usually desirable in order to retard the EVO timing while not penalizing BSFC. Moreover, an exhaust valve faster opening may also reduce the blow-down flow losses increasing the energy available at turbine inlet, especially needed at low engine speed where the variable geometry turbine is usually closed.

*Early Exhaust Valve Closing (EEVC).* In conventional diesel engines, EVC takes place at around 20° after TDC. Advancing this event prevents partially or totally valve overlap, which reduces or avoids the backflow of burnt gases through intake valves. This way, EEVC aids to retain a portion of burnt gases inside the cylinder, which results in a reduction of engine-out NO<sub>x</sub> and HC emissions<sup>4</sup>. Nonetheless, this strategy has some limitation to be applied on passenger vehicles as some authors reported an audible noise when the compressed exhaust gases eject into the intake manifold<sup>12</sup>.

*Late Exhaust Valve Closing (LEVC).* In order to perform LEVC, the exhaust valves are closed well after TDC, increasing the valve overlap period. This long overlap during the intake stroke results in some part of the burnt gases flowing back into the cylinder, creating an internal gas recirculation. Regarding engine-out pollutant emissions, NO<sub>x</sub> and HC emissions are reduced when performing LEVC due to the IGR<sup>4</sup>.

Because of the small clearance height between piston and cylinder head at TDC in CI engines, LEVC and EIVO are quite limited. This is also the reason why the application of VVT is more restricted in CI engines than in SI engines.

At high engine speed, the time in which both valves are opened is less than at low engine speed. In order to provide higher engine power output, a high valve overlap is beneficial for scavenging of residual gases, since the higher inertia of the gases at high engine speed allows removing residual gases from the cylinder and increases volumetric efficiency. But a large valve overlap is detrimental for low engine speed torque due to the larger amount of residual gases flowing back into the intake manifold.

Variable valve timing (VVT) strategies usually consist of a combination of the different sub-strategies mentioned above, like, for instance, phasing the exhaust; which can be a combination of EEVO and EEVC or, on the other side, a combination of LEVO and LEVC. Moreover, there are other different strategies in order to add flexibility to the engine valve train. By modifying valve lift it is also possible to perform different opening-and-closing valve events along the engine cycle. This systems are called as variable valve actuation (VVA).

It is known that IGR can increase the exhaust gas temperature and reduce engine-out emissions. This is done with the aid of a charge composition control achieved by an exhaust valve post-lift (or exhaust valve re-opening, EVrO) or an intake valve pre-lift during the exhaust stroke<sup>6,17</sup>.

Intake valve pre-lift consists of a previous intake valve opening event during the exhaust stroke. The aim is to create a backflow of exhaust gases into the intake manifold that are re-entrained later during the intake stroke. On the contrary, the exhaust valve re-opening consists of a secondary exhaust valve opening event during the intake stroke. The vacuum created by the downward movement of the piston creates a backflow of exhaust gases from the exhaust manifold into the cylinder. Benajes et al.<sup>6</sup> found that the IGR amount achieved is higher when performing an exhaust valve post-lift than in the case of an intake valve pre-lift, with advantage of recirculating the same amount exhaust gases independently of the speed and load.

## Model setup and validation

### *Virtual engine model (VEMOD)*

The gas dynamics software VEMOD<sup>18</sup> has been used for this study. In VEMOD the air management is computed by means of a 1D gas dynamics model which performs the calculations of the flow properties along the intake and exhaust systems as well as the high and low pressure EGR paths. Thus, specific sub-models are considered for the boosting system<sup>19,20</sup>, air-charge and EGR coolers, throttle valves, heat transfer including gas-to-wall heat exchange and wall temperature prediction, after-treatment sub-models (DOC and DPf), a 0D turbocharger model and a hydraulic circuit model. The gas dynamics model is coupled to a cylinder model that predicts the in-cylinder conditions based on the combustion process. Detailed heat transfer model is used to obtain the heat rejection to the chamber walls while mechanical losses model allows obtaining the brake power. An emission sub-model is coupled to the combustion process to predict raw NO<sub>x</sub>, CO, HC, and soot emissions as a function of the engine operating conditions. Figure 2 represents the air path systems present in the virtual engine model.

The turbocharger is based on 0D compressor and turbine sub-models. They use the data provided by the supplier maps for both turbine and compressor to compute the flow and the turbomachine efficiencies at any operating point within the maps. Besides, the model is able to extrapolate outside these maps so it is possible to simulate off-design conditions<sup>20</sup>.

The combustion and emissions sub-model consists of a 1D model able to predict the combustion profile and the main pollutant emissions with an acceptable accuracy. For the sake of completeness, the IMEP relative error is about

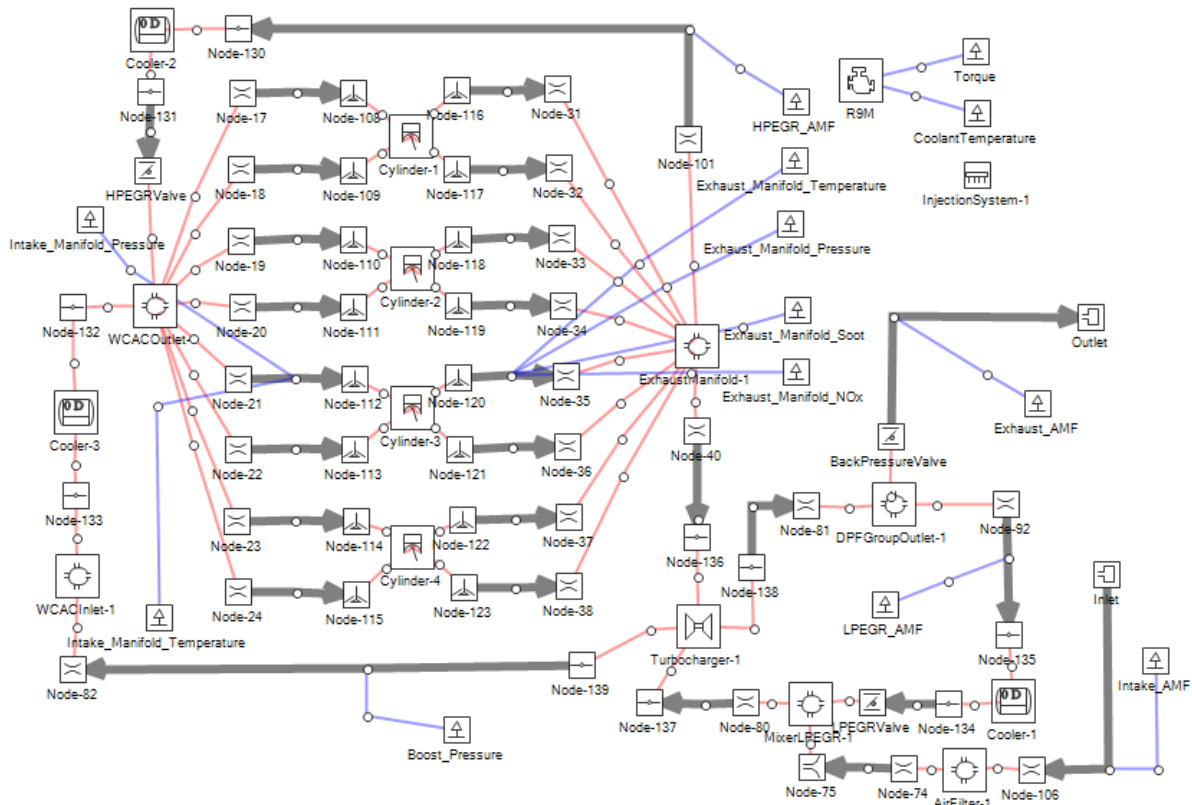


**Figure 2.** Model scheme of the 1D engine model in VEMOD software.

3% and the  $\text{NO}_x$  emissions error is about 8% throughout the WLTC<sup>18</sup>. The combustion model is composed of three main sub-models: ignition delay, premix combustion and diffusion combustion models; along with a 1D model describing the mixing process. A detailed description of the model can be found in<sup>21,22</sup>.

The hydraulic circuits sub-model allows calculating mass flow and temperatures of oil and coolant at different engine components like the engine block galleries, the EGR coolers, the turbocharger and the oil and coolant pumps. Hydraulic circuit elements like thermostats, operable valves, pumps and heat exchangers have been modeled and simulated. Further details regarding the hydraulics sub-models are collected in<sup>23</sup>.

Figure 3 shows the flow-chart of the virtual engine model. The blue boxes represent the thermo and fluid dynamics sub-models described above, while the red boxes represent the different control sub-models, which have been developed in Matlab/Simulink. They operate the engine model by actuating over the different actuators defined in the engine model. The driver and vehicle model can be detached from the control sub-model if just the engine speed and torque setpoints are provided.

Throughout this study, all the simulations were performed keeping the torque of the baseline case, which is the one with original valve events. In order to achieve this objective, a control system included in VEMOD has been used. The control model emulates the ECU to control the injection by modifying the injection pressure, the fuel mass split and the start of injection depending on engine speed and total fueling rate. The model also controls the air loop by means

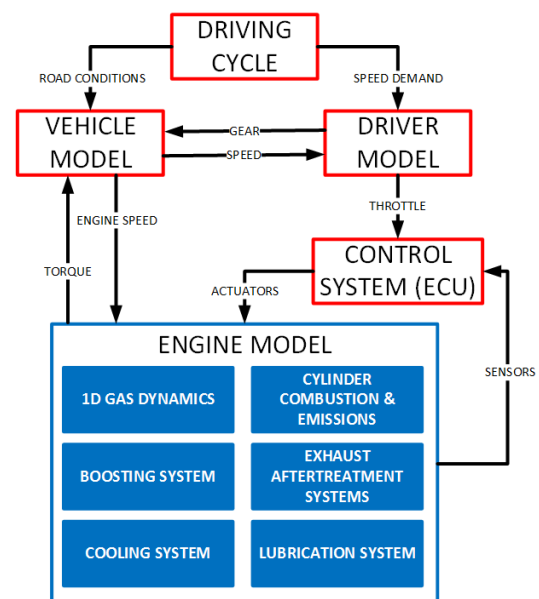


**Figure 3.** Flow-chart of VEMOD modules.

of the VGT rack position (whose control is based on the intake pressure setpoint, depending on engine speed and total fueling rate), and LP-EGR, HP-EGR and back pressure valves, which control is based on the air mass flow setpoint. For any specific engine speed and torque, the required fuel mass is obtained from a calibration map. Once the engine speed and fuel mass are known, the injection pulses timings and masses, intake manifold pressure setpoint, injection pressure and air mass flow setpoints are obtained from their

respective maps. These maps were created on the basis of a series of 23 steady-state points spread throughout the entire engine map and using the baseline valve-train configuration.

The calibration process and the results in terms of burn rate, in-cylinder pressure, mechanical losses, pollutant emissions, as well as detailed information about the different sub-models are described in <sup>18</sup>.

The engine model has been calibrated and validated experimentally in a HSDI Diesel engine. This is a 1.6L four-stroke engine compliant with Euro 5 emissions regulations whose specifications can be found in Table 1. From the point of view of thermal management, the low pressure EGR is cooled by a gas-coolant heat exchanger, and another gas-coolant heat exchanger cools the intake air to the cylinders. In order to reduce the warm-up time, the engine includes an electrovalve that blocks coolant flow through the engine block during engine warming.

**Table 1.** Engine specifications.

Type	EURO 5 HSDI Diesel engine
Displacement	1598 cm <sup>3</sup>
Stroke	79.5 mm
Bore	80 mm
Compression ratio	14.5:1
Number of valves	4 per cylinder (2 intake, 2 exhaust)
Number of cylinders	4 in line
Air management	VGT, LP-EGR, HP-EGR
EAT System	Closed-coupled DOC + DPF
Max. power @ speed	96 kW @ 4000 rpm
Max. torque @ speed	320 Nm @ 1750 rpm

The test cell consists of a climate dynamic room, which allows performing cold start tests (up to -15°C). The test cell is fully equipped to measure operation mean variables and in-cylinder pressures in the four cylinders. It also includes a Horiba MEXA-One exhaust gas analyzer along with an AVL439 Opacimeter. Table 2 summarizes the relevant instruments used for this study. Data was acquired at a frequency of 10Hz with a test automation system.

**Table 2.** Test cell instrumentation.

Variable	Instrument	Range	Accuracy
Crank angle	Encoder	0-360°	±0.02°
Torque	Dynamometer	0-400 Nm	±0.5 Nm
Gas/wall temperature	k-type thermocouple	70-1520 K	±2 K
Air mass flow	Sensyflow DN80	0-1700 hg/h	±2 %
Coolant flow	Krohne 400 Optiflux	4.5-90 L/min	±0.5 %
Oil pressure	Piezoresistive transducer	0-10 bar	±25 mbar
In-cylinder pressure	AVL GH13P	0-200 bar	Linearity 0.3 %

In Figure 4 several variables are represented comparing experimental measurements against model results. Figure 4a shows engine brake torque with a coefficient of determination ( $R^2$ ) of 0.955. During low speed part of the WLTC, when HP-EGR is enabled, model shows low torque peak values. This is a consequence of a lower air mass flow target reached by the air loop controller during the HP-EGR

activation period, since the air mass flow setpoint is obtained from a calibration in which there is no HP-EGR flow, so the corresponding air target at a specific speed and torque slightly differs from the real one. Consequently, intake air mass flow is slightly lower in this period. Once HP-EGR is disabled, brake torque seems to match experimental one until the end of the test cycle; since air mass flow target is fulfilled and fuel mass is always imposed.

Figure 4b shows the turbine outlet temperature, which coincides with the gas temperature at DOC inlet. Although no after-treatment model has been included in this study, it is interesting to analyze how different VVT strategies affect EAT inlet temperature, particularly during the warm-up time. The faster the light-off temperature on the catalyst is reached, the faster the efficient oxidation of CO and HC, and the oxidation of NO to NO<sub>2</sub>, is achieved. The decrease in DOC-out NO<sub>2</sub> can have a negative effect on downstream NO<sub>x</sub> abatement, specially at temperatures below 250°C, such as those at engine start up<sup>24</sup>. Moreover, DOC conversion efficiency increases as the temperature grows<sup>25,26</sup>, so an increment in DOC inlet temperature can be profitable. The model is able to follow well the turbine outlet temperature trend, specially during the medium and high speed part of the WLTC.

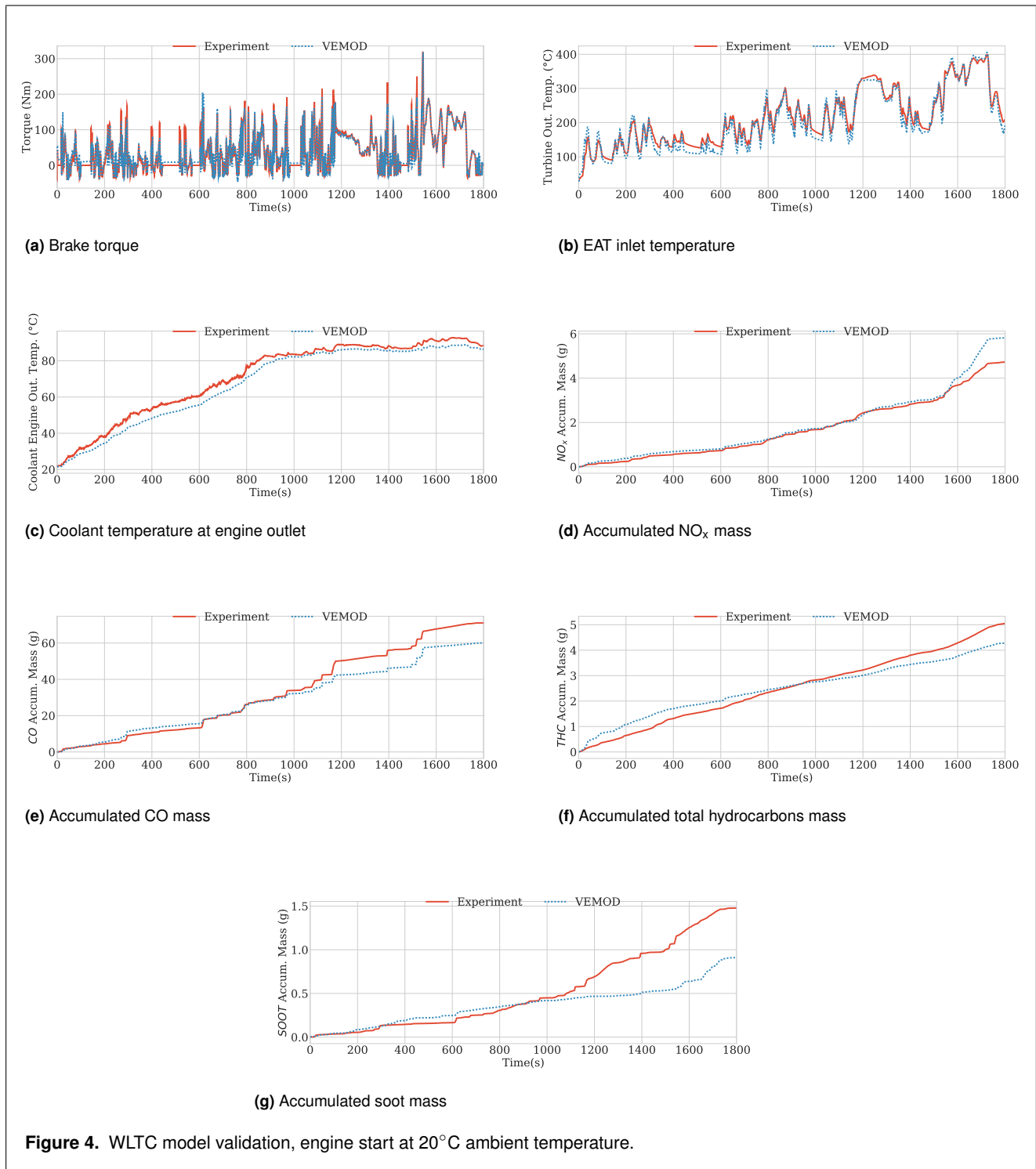
Coolant temperature at cylinders outlet is shown in Figure 4c. In this case, a medium total error of -2°C along the whole cycle was obtained. Since the coolant temperature has a slight effect on the volumetric efficiency and consumption, and some effect on NO<sub>x</sub> formation<sup>27,28</sup>, it is interesting to achieve a good prediction. According to the authors, an increase in the coolant temperature leads to an increment of the cylinder wall temperature, which increases the air temperature during the intake stroke, and results in a decrease of the air density. This cylinder wall temperature increment also has some impact on the NO<sub>x</sub> formation, specially at low load<sup>28</sup>.

Figure 4d and Figure 4e show NO<sub>x</sub> and CO accumulated emissions at engine outlet, right upstream the after-treatment system. In both cases, the overall formation is well reproduced along the WLTC. However, CO formation prediction is more accurate than NO<sub>x</sub> one, which is overestimated. This overestimation is shown very clearly during the high speed stretch of the WLTC, where NO<sub>x</sub> formation increases.

Regarding hydrocarbons, Figure 4f shows a good prediction of total HC at engine outlet. It can be seen a little overestimation at the beginning of the cycle. Contrarily, the model underestimates the THC emissions formation at high speed and high load. The soot formation model, Figure 4g, provides an accurate prediction up to 1100s. After this time, the model clearly underestimate the soot formation.

### Variable valve timing strategies

Several variable valve timing strategies were tested. The first two strategies consisted on phasing exhaust timings (“Exhaust phasing” and “EEVO + dwell”). The third strategy consisted on phasing both intake and exhaust timings (“IP + EP”), whilst the last two strategies consisted on performing an exhaust valve re-opening modifying the re-opening lift and duration. Intake and exhaust valve lifts according to each strategy are shown in Figure 5.



- **Baseline cams:** Corresponds to the original cam valve timing (black dashed line in Figure 5). In this case, EVO and EVC are located at 107° and 396°, respectively from combustion TDC. Regarding intake valve timing, IVO and IVC take place at 326° and 602° respectively from combustion TDC as well.
- **Exhaust phasing and Intake phasing (EP + IP):** This strategy corresponds to a combination of both a Early Exhaust Valve Opening (EEVO) and a symmetrical Later Intake Valve Opening (LIVO). In this case, valve profiles' duration for both intake and exhaust valves were not modified (dark red solid line in Figure 5),

this means that both profiles were phased and EVC and IVC instants were phased as well. Three different configurations were tested by advancing EVO and EVC, and delaying IVO and IVC simultaneously, 20°, 30°, and 40°. A fourth configuration advancing exhaust/delaying intake 60° was tested resulting in a dramatic drop of torque.

- **Exhaust phasing:** This strategy is quite similar as the previous one with the difference that intake valve timings were not modified. As in “EP + IP” strategy (green dashed line with cross markers in Figure 5), three configurations were simulated (20°, 30°, and

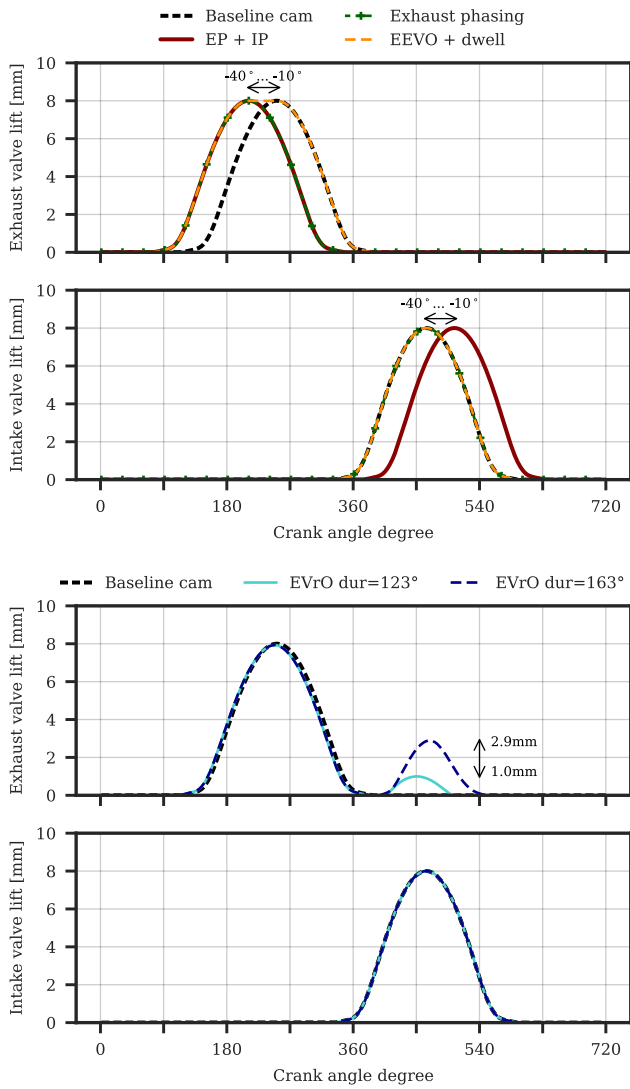


**Figure 5.** Exhaust and intake valve lift profiles for each configuration.

40°) by advancing the entire exhaust valves profiles. Again, an exhaust valve phasing of 60° was found to be excessive due to the drop of torque and power output.

- **EEVO + dwell:** Represented by an orange dashed line Figure 5, EVO instant was advanced 20°, 30°, and 40°, but keeping unchanged the EVC instant. The opening and closing slopes are kept; as a result, there is an angle interval in which the exhaust valves are fully opened. This angle interval will be called “dwell” along this study.
- **EVrO:** Exhaust Valve re-Opening strategy consists of performing a second exhaust event (also called post-lift or re-breathing in literature) during the intake stroke. For this study two different strategies were tested. On the one hand, a second exhaust event that lasts for 163° (from 392° to 555°) and three different valve lifts (1.0 mm, 2.0 mm and 2.9 mm) were tested. It is represented by a blue dashed line in Figure 5. On the other hand, an analogous strategy was tested with the same three different valve lifts but with a shorter re-opening, 123° (from 392° to 515°) instead of 163°.

This re-opening strategy is represented by a light blue solid line in Figure 5. The exhaust valve re-opening was performed only in one of the two exhaust valves, keeping the original cam profile in the other valve.

Table 3 summarizes the strategies described above.

**Table 3.** Variable valve actuation strategies.

	VVT Strategies				
	EP + IP	Exhaust phasing	EEVO + dwell	EVrO 163	EVrO 123
IVO (°)	326 + [20, 30, 40]	326	326	326	326
IVC (°)	602 + [20, 30, 40]	602	602	602	602
EVO (°)	107 - [20, 30, 40]	107 - [20, 30, 40]	107 - [20, 30, 40]	107	107
EVC (°)	396 - [20, 30, 40]	396 - [20, 30, 40]	396	396	396
2nd event lift (mm)	-	-	-	1.0, 2.0, 2.9	1.0, 2.0, 2.9
2nd event duration (°)	-	-	-	163	123

Notes: Angles starting from the combustion TDC. EVrO applied only to one of the two exhaust valves.

## Results and discussion

In order to perform this study, the resulting torque from the baseline cam simulations was imposed as the torque target for all the different strategies. The ECU control model basically takes control on the fuel mass injected and the required air mass flow to reach the torque at any operating point, based on the baseline engine calibration that contains several maps for boost pressure, air mass flow and fuel injected. In this way, it is possible to quantify differences on fuel consumption, pumping losses, exhaust temperature and other key outputs when compared to the baseline configuration.

### Steady-state analysis

A total of 23 operating points were tested for each strategy; however, a representative sample is discussed in this study taking a pair of points at 1000 and 1500 and partial loads. These points, shown in Table 4, were measured experimentally without any modification on the engine valvetrain, so these points are included in the calibration used by the ECU model. Moreover, the selected points represent a sample of the low speed stretch of the WLTC, whose transient results will be discussed on the next section. It should be noted that any full load point is included in this steady-state analysis. The justification is that the ECU control is not able to reach, in some cases, the torque target



without exceeding the full load fuel limit included in the calibration. In most of the configurations it is impossible to do an iso-torque comparison at full load, specially when the exhaust is advanced more than  $40^\circ$  at full load and also when performing a exhaust re-opening. At some operating points, when performing a second exhaust valve event “EVrO  $163^\circ$ ”, the control is not able to fulfill the torque target. Those points have been removed from the following figures in order to show an iso-torque comparison.

**Table 4.** Simulated steady-state operating points.

Engine speed (rpm)	BMEP (bar)	Torque (Nm)
1000	1.9	23.9
1000	5.9	75.4
1500	2.4	30.9
1500	5.1	64.7

Figure 6 and subsequent figures on this section show the steady state results for four different operating points (Table 4). Several representative variables are presented in different subfigures comparing the results obtained by each VVT configuration. The values presented have been normalized according to the baseline configuration results, so all the figures (except from turbine outlet temperature, which shows absolute difference in Celsius degrees) represent percentage variations respect to the baseline results.

Figure 6 shows the steady-state results for a low speed and low load operating point (1000 rpm and 1.9 bar in BMEP). The specific fuel consumption (BSFC) variation in Figure 6a, in terms of percentage, points that all the configurations incur in a penalty in fuel economy. Furthermore, it can be inferred that the increment in exhaust temperature is proportional to the fuel consumption. This trend has been observed in all the four cases, as shown in Figure 6a, Figure 7a, Figure 8a and Figure 9a. For the case of “EEVO + dwell” strategy, it can be seen that the temperature increase achieved is about  $20^\circ$  in the best case (1500 rpm and 5.1 bar in Figure 9), resulting in the worst strategy to increase the inlet DOC temperature. The justification for this effect is that, since EVC remains unchanged, no additional amount of exhaust gases is retained in the cylinder for the next cycle. As a result, the entrained gas temperature after the IVC is slightly lower than in the baseline case, leading to an insignificant increment in the exhaust gases temperature for the studied cases. A higher increment in the exhaust temperature (about  $30^\circ\text{C}$ ) can be achieved by the “EEVO + dwell” strategy by advancing  $67^\circ\text{CA}$  before TDC. However, the fuel penalty in BSFC goes beyond 20% in most of the cases. This behavior is explained by the early exhaust blowdown, which produces an inefficient engine operation due to the higher fuel amount injected<sup>15</sup>.

As far as pollutant emissions are concerned, even though “EEVO + dwell” strategy does not have a relevant effect on the exhaust temperature, it shows an identifiable trend in  $\text{NO}_x$  formation reduction as the engine speed increases and engine load decreases (Figure 6b and Figure 8b). The explanation to this phenomenon resides in the fast drop of the cylinder temperature towards the middle of the expansion stroke, which results in less residence time of the burnt gases at high temperature. This residence time is lower as the engine speed increases and, besides, it is even lower for greater EEVO. A

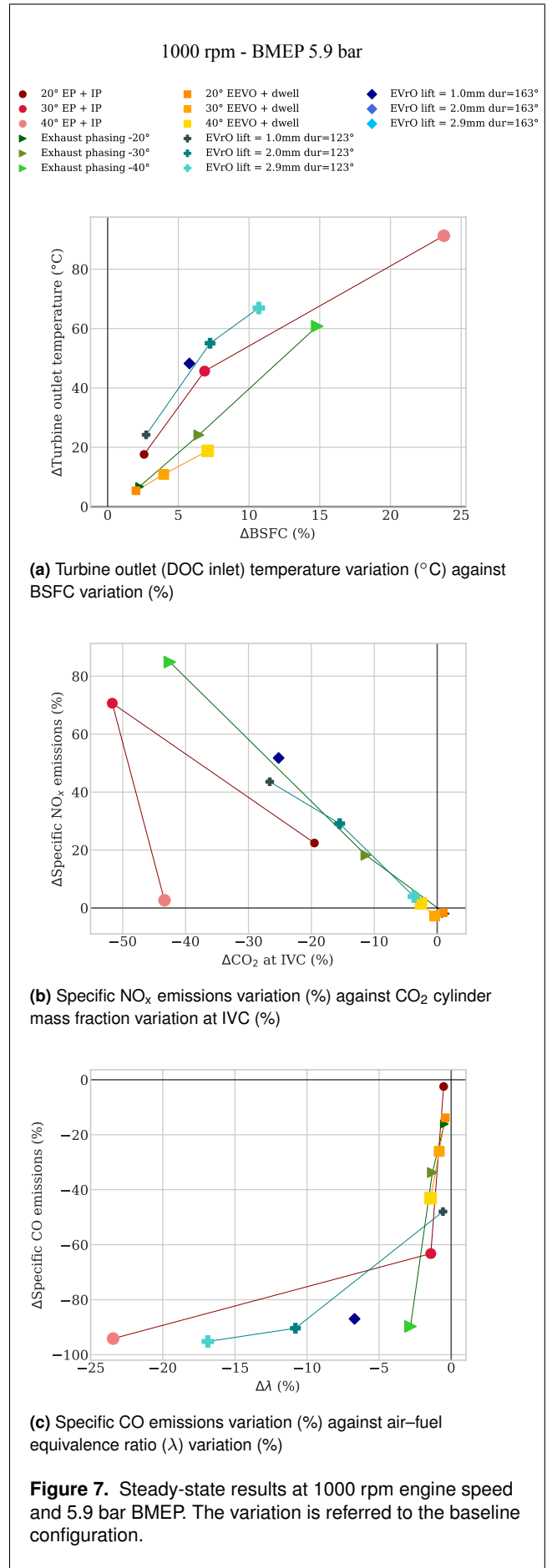
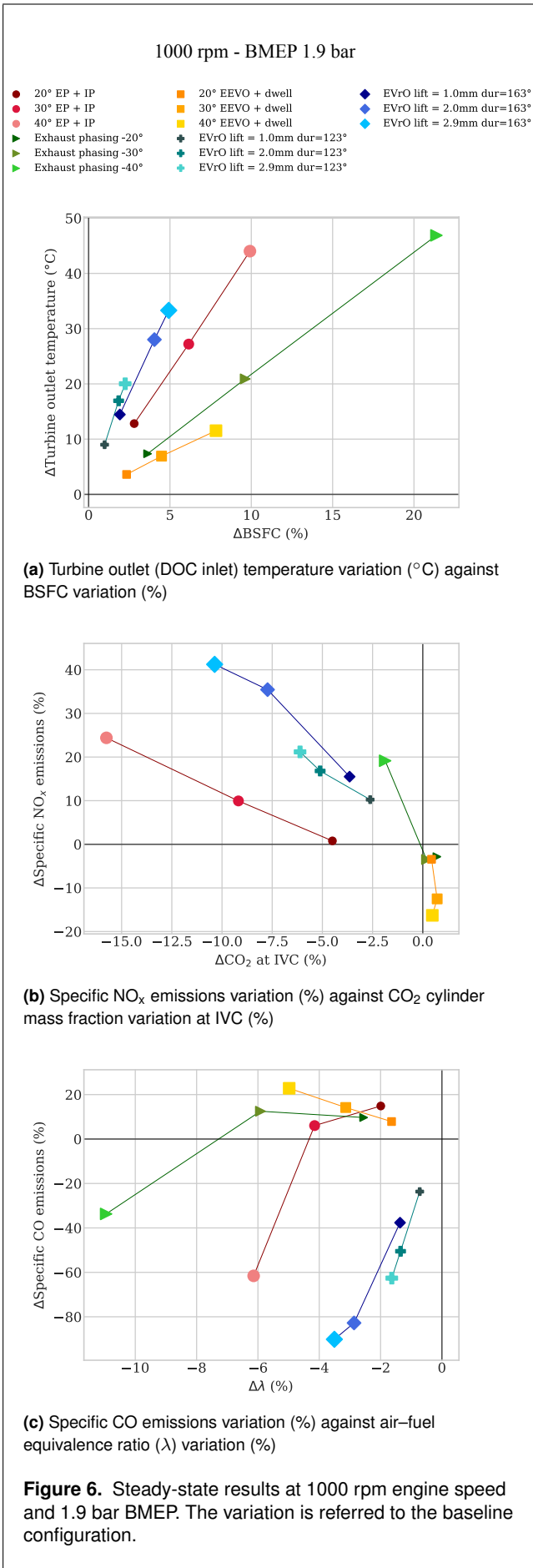
similar trend can be observed also for the CO formation, it reduces as engine load decreases (Figure 7c and Figure 9c). In this case the conversion of HC into CO is interrupted as EVO is advanced, resulting in a reduction of CO emissions when compared to the baseline case. It is worth to mention that, due to possible uncertainties in the pollutants formation model, this emissions analysis is focused on trends more than in specific amounts.

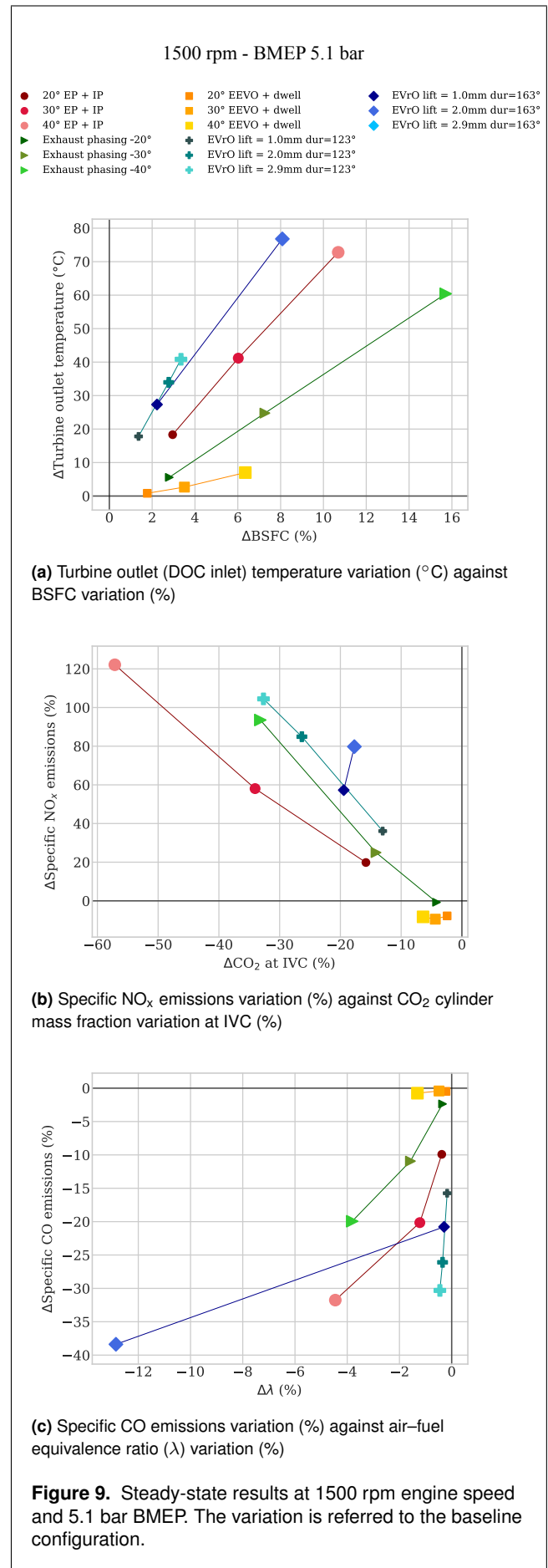
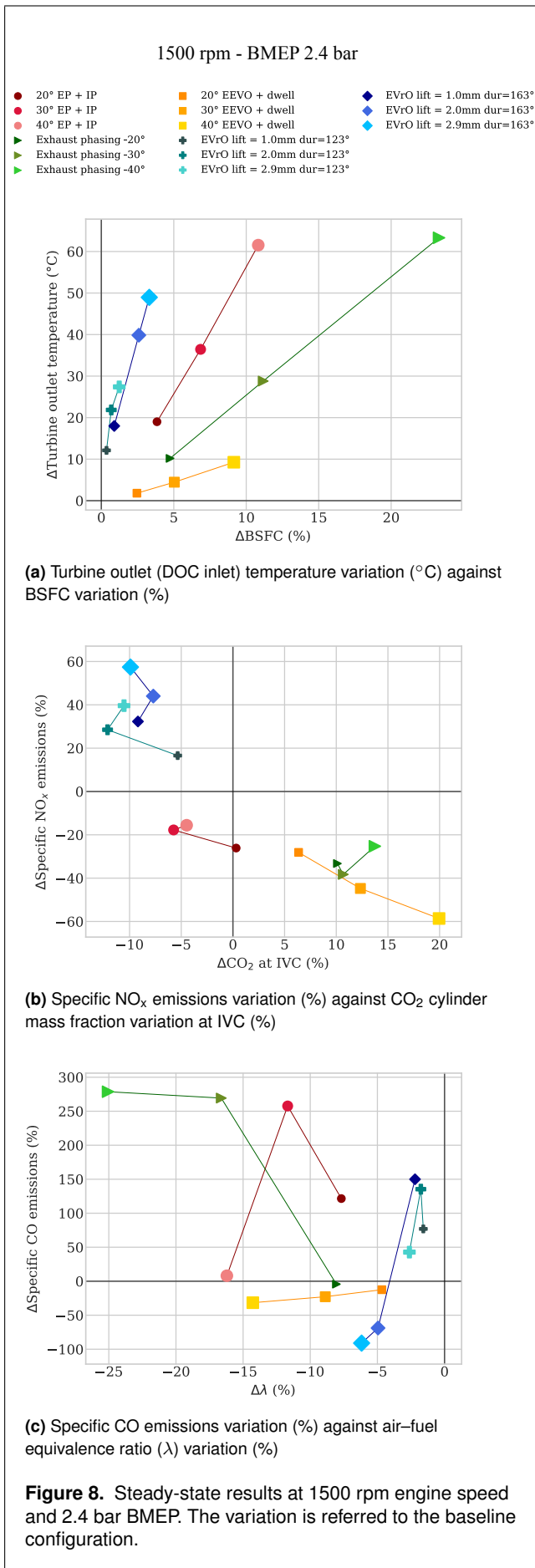
The “EVrO  $123^\circ$ ” strategy offers a good potential when heating the exhaust gases, specially above 5 bar BMEP. Furthermore, the greater the maximum lift during the post-lift, the greater the temperature increment in all cases. This strategy presents another advantage: its penalty in fuel economy is not so high compared with other strategies: the increment in BSFC is below 4%, although a maximum of 11% is reached at 1000 rpm 5.9 bar BMEP (Figure 7a) with the maximum lift (2.9 mm).

On the other side, the “EVrO  $163^\circ$ ” strategy achieves a higher increase in exhaust temperature compared to the “EVrO  $123^\circ$ ”, but leading to a slightly higher fuel consumption. The main drawback is that “EVrO  $163^\circ$ ” with a 2.9 mm maximum lift is not able to fulfill the torque demand in most of the cases (5 bar BMEP and above), since the control tries to provide more fuel before reaching the stoichiometric air-fuel ratio. These points have been removed as explained above, since they do not offer a fair comparison (Figure 7 and Figure 9). Nonetheless, the configuration whose maximum lift is 1 mm always able to reach the torque target, obtaining an exhaust temperature increment between  $10^\circ\text{C}$  and  $30^\circ\text{C}$ ; concluding that a short re-opening (“EVrO  $123^\circ$ ”) is more profitable at medium and higher loads than the “EVrO  $163^\circ$ ” version in terms of exhaust enthalpy.

Analyzing  $\text{NO}_x$  emissions when performing an exhaust re-opening it can be observed that emission levels are higher in all the four operating points compared to the baseline case. Exhaust  $\text{NO}_x$  specific emissions increase with the maximum lift reached during the re-opening and the increment is higher than 50%. The lower  $\text{CO}_2$  mass fraction at IVC, which indicates less residual mass in the combustion chamber, leads to greater maximum temperatures during the combustion which increases the  $\text{NO}_x$  formation. This trend applies to both “EVrO  $163^\circ$ ” and “EVrO  $123^\circ$ ” strategies, with slightly less  $\text{NO}_x$  formation in the “EVrO  $123^\circ$ ” case (an increment around 30% when the maximum lift is equal to 1 mm).

Regarding CO formation, a potential reduction can be observed in Figure 6c, Figure 7c, Figure 8c and Figure 9c for all the presented points (more than 50% for some of them), specially at 1000 rpm. The lean mixture (even though  $\lambda$  is lower than in the baseline case because of the higher fuel mass, there is lower EGR flow than in the baseline case Figure 8b and Figure 9b) that can be achieved by applying EVrO results in lower CO pollutant emissions. This trend is observed for both EVrO strategies being magnified in the  $163^\circ$  re-opening duration cases. The maximum re-opening valve lift also plays a role in the CO reduction, leading to lower emissions when increasing the lift. When the re-opening lift and duration are higher, the residual trapped mass is too high and leads to low oxygen mass in the combustion chamber. Therefore, all the carbon cannot be converted to  $\text{CO}_2$  during the combustion and more CO is formed.





“EP + IP” strategy allows reaching the greatest increase in exhaust temperature in most of the cases when intake and exhaust are phased  $40^\circ$ . The fuel penalty is around 5% to 10%, but it is higher when increasing the engine load: (15%) when intake and exhaust are phased  $40^\circ$ . The higher fuel consumption compared to the re-opening strategies is due to the compression of the retained burned gases after the EVC, since this compression increases the pumping losses and thus the BSFC. The earlier EVO also affects fuel economy as it reduces the power stroke and increases the amount of fuel injected to keep the required torque. This increase in fuel consumption is also observable in “Exhaust phasing” and “EEVO + dwell” strategies. In the “Exhaust phasing” strategy the increase in exhaust temperature also increases with the greater advance in the exhaust event, in this case with an exhaust temperature increment about  $5^\circ\text{C}$  to  $20^\circ\text{C}$  below the one achieved by the “EP + IP” strategy. The temperature difference between these two strategies increases with the load, as can be seen in Figure 7a and Figure 9a. This difference, when the exhaust is advanced by  $40^\circ$ , is due to the higher fuel-air ratio when performing “EP + IP”, since air mass flow is lower than the baseline case whilst fuel required is higher. Contrarily to the exhaust temperature difference, BSFC is higher in “Exhaust phasing” strategy due to the compression of the burned gases after the advanced EVC, which increases pumping losses. In “EP + IP”, this compression is followed by an expansion of the burned gases due to the later intake, resulting in a lower penalty in fuel consumption.

In case of “EP + IP” strategy, and upward trend is observed in  $\text{NO}_x$  formation as engine load increases. The increment on  $\text{NO}_x$  formation compared to the baseline case can be explained because of the lower EGR mass flow when increasing the engine load as indicated by the  $\text{CO}_2$  mass fraction at IVC in Figure 7b and Figure 9b. The higher intake fresh air mass flow, coupled with an increase in fuel consumption, leads to higher in-cylinder temperatures and, thus, producing more  $\text{NO}_x$ . At 1000 rpm and 5.9 bar BMEP it can be observed how the richer mixture achieved by “ $40^\circ$  EP + IP” strategy results in a great reduction in  $\text{NO}_x$  emissions compared to the  $30^\circ$  version in Figure 7b. An opposite trend can be observed for CO pollutant emissions due the lower residual burned gases retained during the combustion. Figure 7c and Figure 9c. At low engine load, however, the  $\text{NO}_x$  formation is reduced for “EP + IP” and “Exhaust phasing” strategies due to a greater ability to retain some residual gas. This effect is more evident at 1500 rpm rather than at 1000 rpm as can be observed in Figure 8b, where a 30% reduction in  $\text{NO}_x$  can be achieved with a 12% more  $\text{CO}_2$  after IVC by the “Exhaust phasing”. On the contrary, higher CO emissions are produced due to the reduction in intake fresh air flow and the increment in fuel consumption (Figure 8c).

Regarding pollutant emissions formation by applying the “Exhaust phasing” strategy, its behavior is similar to “EP + IP” strategy.  $\text{NO}_x$  formation increases with the engine load and is higher for greater advances in EVO and EVC. Keeping the baseline intake timing leads to  $\text{NO}_x$  formation values that are slightly lower compared to “EP + IP” strategy. This difference is explained by the higher IGR achieved by “Exhaust phasing”, specially at low load (Figure 8b). In

terms of CO formation, the trend is similar in both strategies and opposite to  $\text{NO}_x$  formation, as explained above.

### Transient analysis

As part of the comparison between the exposed VVT strategies, a transient analysis has been carried out taking the first low vehicle speed part of the WLTC (589 seconds) as reference. This phase of WLTC has been selected in order to evaluate the potentials at cold start of each strategy.

Recent studies carried out by Deppenkemper et al.<sup>7</sup> found that, in an engine with similar specifications, the light-off temperature of the DOC is around  $200^\circ\text{C}$  according to an averaged space velocity of 57700 l/h during the WLTC<sup>7</sup>. Other authors like Guardiola et al.<sup>29</sup> take this temperature as a reference the DOC light-off temperature. In order to evaluate the temperature downstream the DOC, a catalyst model<sup>25</sup> has been included into the engine model. Currently, the DOC model is able to predict the pressure drop and the heat transfer through the monolith. Thus, it is possible to compare the resulting DOC outlet temperature among the different VVT strategies, since the gas temperature is similar as the one in the channels wall. Looking at Figure 10a, it can be observed that only “EP + IP” and “Exhaust phasing” achieve a faster DOC heat-up compared with the baseline configuration when the phasing is higher than  $20^\circ\text{CA}$ . The greater time reduction is achieved by the “Exhaust phasing” strategy which allows a reduction of 74 seconds. Regarding “EEVO + dwell”, there is no DOC heat-up improvement since this strategy does not produce an important increment in the exhaust temperature (with the current EVO advances) as seen in Figure 10b. Both exhaust valve re-opening strategies increase the DOC heat-up time as the second event maximum lift increases. Although EVrO can increase the DOC inlet temperature (Figure 10b) the fact is that in the transient accelerations where the model is unable to reach the torque target, such as the EVrO with a lift higher than  $1\text{mm}$ , the resulting peaks in the temperature downstream the turbine are not reached; thus, the DOC is not heated as quickly as in the baseline case. Consequently, the time to reach DOC light-off temperature increases in these cases. The same situation is observed in the “EP + IP  $30^\circ$ ” case, where the time to reach DOC light-off temperature increases compared to its  $20^\circ$  case.

Figure 10b shows the exhaust mass averaged temperature downstream the turbine during the low speed phase of the WLTC. Relevant information is derived from this comparison. On the one hand, all the strategies show an increment in the exhaust temperature, as it was expected. “EEVO + dwell” performs poorly as it was shown in the steady-state analysis. On the other hand, both “EP + IP” and “Exhaust phasing” strategies perform better than EVrO ones, showing an average increment of  $6^\circ\text{C}$  to  $34^\circ\text{C}$  when advancing the exhaust and  $10^\circ\text{C}$  to  $27^\circ\text{C}$  when also delaying the intake. “EVrO  $163^\circ$ ” option shows a greater potential when heating the exhaust than the “EVrO  $123^\circ$ ” variation. Their highest average temperature values are  $144^\circ\text{C}$  and  $138^\circ\text{C}$ , respectively. The increase in the exhaust temperature follows a trend that is consistent with time needed to heat the DOC inlet: the increment is higher when earlier the EVO. In case of performing a second exhaust valve event, there is an increment in the exhaust temperature, but this temperature

results in being lower than the baseline's one in the higher speed peaks of the transient cycle.

Coolant temperature plays an important role in the engine warm-up as well as in the low pressure EGR activation. Heating up the engine increases its efficiency during the heating phase. During this time the coolant thermostat is closed, so the coolant temperature keeps raising until a determined value is achieved. Figure 10c shows the time required to heat the coolant up to 70°C. It can be observed that all the strategies meet the goal of heating the coolant quicker than the baseline case. This way, except from the "Exhaust phasing" cases, a warm-up time reduction between 10 to 25 seconds can be achieved with the "EP + IP", "EEVO + dwell" and "EVrO 163°" strategies. However, the fastest warm-up time can only be achieved by the "Exhaust phasing" strategy. The fact that the compression of the trapped exhaust gases after the EVC is not followed by an expansion like in the "EP + IP" cases, leads to a hot backflow of exhaust gases that is expelled into the intake ports at IVO; thus, resulting in a heating of the coolant that surrounds the intake ports. In this case, it is possible to reduce the warm-up time by 93 seconds.

Regarding fuel consumption, Figure 10d shows the accumulated fuel consumption throughout the first 589 seconds of the WLTC. As it was mentioned above in the steady-state analysis, all the strategies incur in a penalty in fuel economy. It can be seen that EVrO strategies offer the lowest penalty in fuel consumption, which is about 7 g (3.8%) more than in the baseline cam case. Advancing the exhaust valves opening increases the fuel consumption in order to keep the target torque. This increment stands out in the "Exhaust phasing" cases due to the higher pumping losses which results in a penalty in fuel consumption increase around 29 g (16.6% for the worst case) compared to the baseline case.

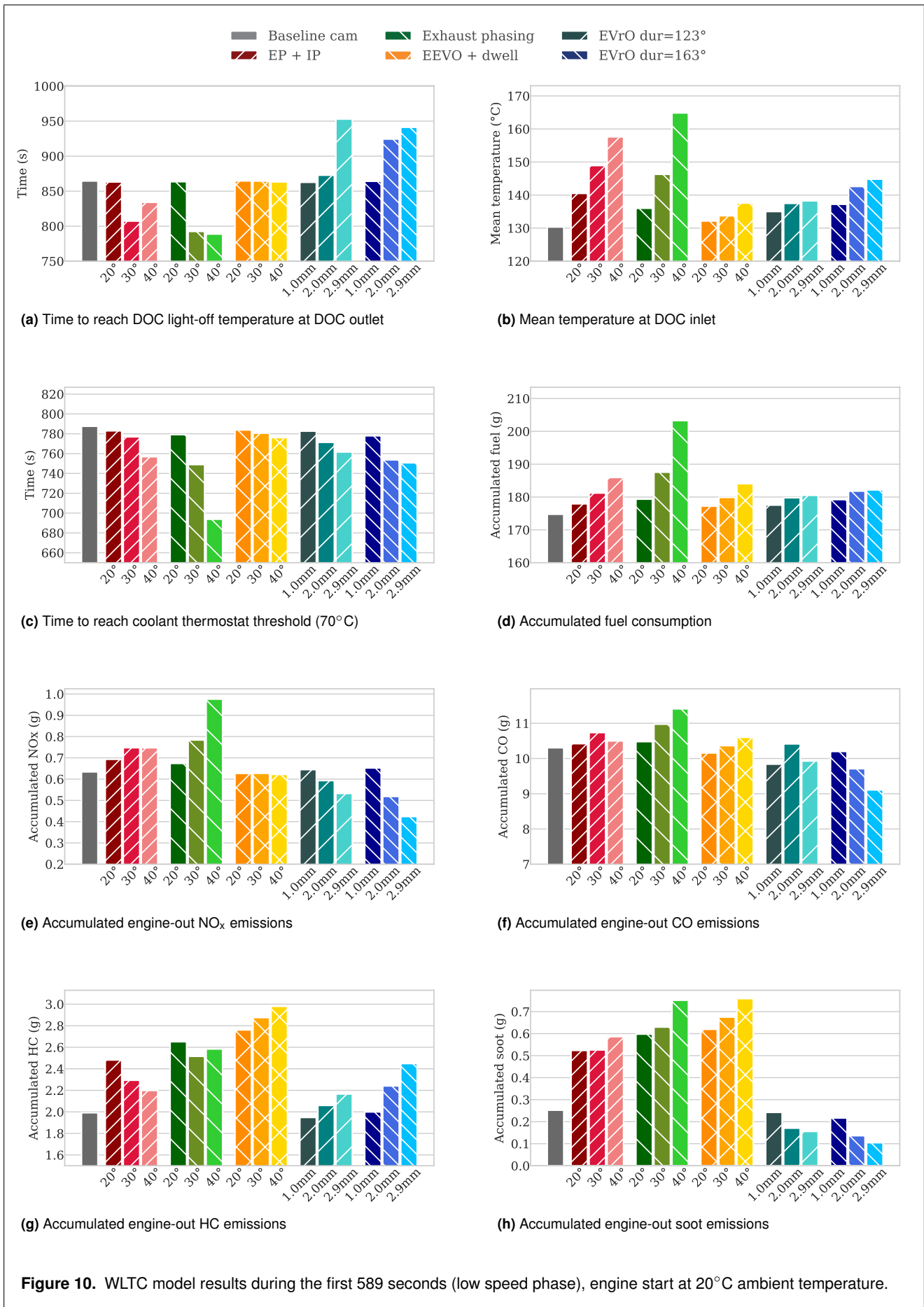
As far as pollutant emissions are concerned, a reduction in NO<sub>x</sub> engine-out emissions is only achieved by performing an exhaust valve re-opening. Looking at Figure 10e, the greater the maximum re-opening lift, the lower the NO<sub>x</sub> formation. This trend is higher in the "EVrO 163°" cases whose 2.9 mm configuration reaches a total of 0.43 g along the low speed phase of the WLTC, a 29% reduction. Although these values could be contrary to the values shown in Figure 6b and Figure 8b, the fact is that the exhaust valve re-opening allows retaining part of the exhaust gases within the cylinder and, consequently, reducing NO<sub>x</sub> formation, whereas in the baseline case there is no low pressure EGR during the low speed phase of the WLTC. Furthermore, during the accelerations, the ECU closes the HP-EGR valve, but the exhaust re-opening still produces IGR during these transients which results in lower peak exhaust temperatures during the accelerations and a reduction in NO<sub>x</sub> emissions. The fact that peak torque values are not reached with the "EVrO 163°" strategy also affects the NO<sub>x</sub> comparison with the baseline case, since the fresh air charge gets reduced and the ECU control limits the fuel injected to prevent a high smoke formation. In case of advancing EVO, the increment in NO<sub>x</sub> emissions is due to a low IGR during the fast accelerations of the WLTC, which means lower burned residual gas mass than in the baseline case. Consequently, the IGR effect that could reduce NO<sub>x</sub> emissions during idle periods and slower

accelerations is not remarkable. In this case the transient results are consistent with the steady-state results, leading to higher emissions as greater is the advance in the exhaust. "Exhaust phasing" achieves the highest NO<sub>x</sub> accumulated amount, 0.94 g which represents an increase of 56%.

Regarding CO (Figure 10f), hydrocarbons (Figure 10g) and soot (Figure 10h) formation, similar trends can be observed. A particular difference can be found in case of the "EEVO + dwell" strategy, whose HC and soot accumulated amounts are high taking into account its low potential in order to heat up the exhaust gases. The greater values are explained due to the fact that performing an EEVO results in an increase in fuel injected mass, which leads to an increment in HC, CO and soot. Moreover, the earlier blowdown interrupts the oxidation of HC and CO during the expansion stroke<sup>4</sup>. Different trends can be observed for HC emissions in "EP + IP" and re-opening strategies. On the one hand, "EP + IP" HC emissions are higher than the baseline case due to the EEVO, but they become lower as greater the LIVO because of the increase in inlet air velocity enhances in-cylinder turbulence, which improves the mixing process, and due to the retention of the hydrocarbon-rich quench gases normally expelled at the end of the exhaust stroke<sup>4</sup>. On the other hand, HC emissions increase as higher is the maximum lift during the re-opening, specially for the longer "EVrO 163°" cases, due to the lack of oxygen as engine load increases for low engine speeds, which results in hydrocarbons not burned.

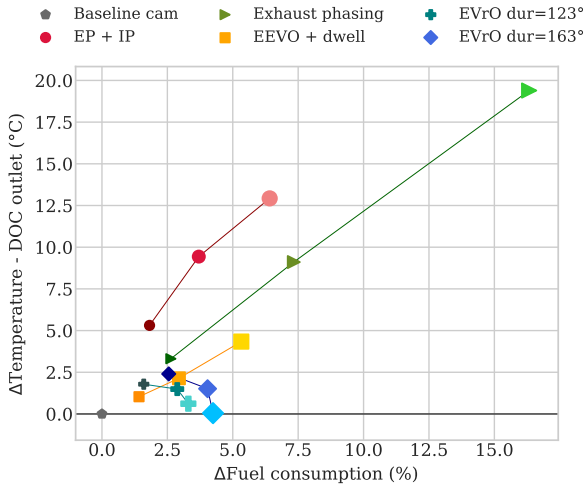
In terms of soot formation, the increase in fuel consumption in "EP + IP", "Exhaust phasing" and "EEVO + dwell" strategies leads to a higher soot production. In case of "EVrO 123°" and "EVrO 163°", the reduced fuel penalty and the reduction in the in-cylinder maximum temperature leads to a lower soot emissions.

Figure 11 shows a performance comparison of all VVT strategies in terms of the increase in the DOC outlet temperature versus the corresponding penalty in fuel consumption during the low speed phase of the WLTC, so this figure summarizes the information shown in Figure 10d and Figure 10b but normalized respect to the baseline values. It can be observed that "Exhaust phasing" achieves the higher increase in temperature (19°C with a fuel penalty of 16%). However, "EP + IP" strategy performs better than "Exhaust phasing" since it can reach around 13°C in less than half the fuel penalty produced by the "Exhaust phasing" strategy. EVrO configurations present a poor performance in this sense, since they do not offer a temperature increase according to the increasing re-opening valve lift. Contrarily, both EVrO strategies offer an increment in DOC inlet temperature that performs between "Exhaust phasing" and "EP + IP" alternatives. The reason to this, as stated before, is because during the transient accelerations where the EVrO strategies (2.0 mm and 2.9 mm) are unable to reach the torque target, the resulting peaks in the temperature downstream the turbine are not reached. Thus, EVrO curves in Figure 11 drop as increasing the lift since the DOC is not heated as quickly as in the baseline case. Figure 12 reflects this situation in terms of time required to reach DOC light-off temperature. It can be observed how this time increases above 75 seconds for the two EVrO strategies.



**Figure 10.** WLTC model results during the first 589 seconds (low speed phase), engine start at 20°C ambient temperature.

According to Figure 12 “EEVO + dwell” strategy do not achieve a faster DOC heat-up no matters the proposed EVO advances. In case of “EP + IP” and “Exhaust phasing”, a 30°CA phasing seems optimal for heating-up the DOC (57 s and 74 s less than the baseline case, respectively), since a greater phasing only deteriorates fuel economy.



**Figure 11.** Fuel consumption variation (%) against mean DOC outlet temperature difference (°C) comparison for all the VVT strategies, taking the baseline case as the reference.

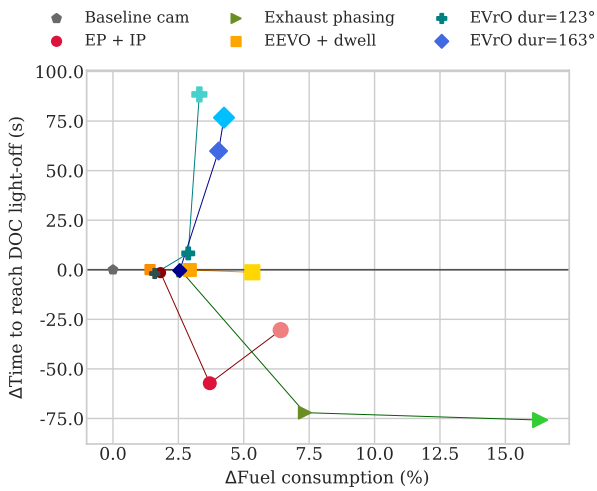


**Figure 12.** Fuel consumption variation (%) against DOC light-off time difference (s) comparison for all the VVT strategies, taking the baseline case as the reference.

On the subject of fuel consumption and emissions trade-off during the WLTC low speed phase, Figure 13 and Figure 14 show the fuel consumption (in %) against NO<sub>x</sub> and CO, respectively, variation with respect to the baseline valve timings. “Exhaust phasing” strategy shows the worst trade off both in NO<sub>x</sub> and CO, whose emissions increase with the fuel penalty. Advancing the exhaust and delaying the intake (“EP + IP”) results in a better trade-off, since NO<sub>x</sub> and CO levels do not increase for a phasing greater than 30°. In this case, a 19% maximum increase in NO<sub>x</sub> is observed with a 3% increment in fuel consumption, while a 4.5% maximum increase in CO is observed with a fuel penalty of 3.7%. “EEVO + dwell” presents a trade-off similar to

“Exhaust phasing”: CO emissions and fuel penalty increase with the earlier EVO; however, there is no variation in NO<sub>x</sub> emissions. Regarding EVrO strategies, both offer a good trade-off in terms of NO<sub>x</sub> and fuel consumption. NO<sub>x</sub> emissions wane as higher the re-opening lift, reaching a -18% change with a 3% fuel penalty in “EVrO 123°” strategy. On the other hand, CO emissions increase quickly with the re-opening lift (from -5% to 1% in “EVrO 123°”). The fall in both NO<sub>x</sub> and CO emissions when increasing the re-opening lift is due to the lower torque achieved by this strategies during the transient accelerations, since the fresh air charge gets reduced and the ECU control limits the injected fuel to prevent a high smoke formation.

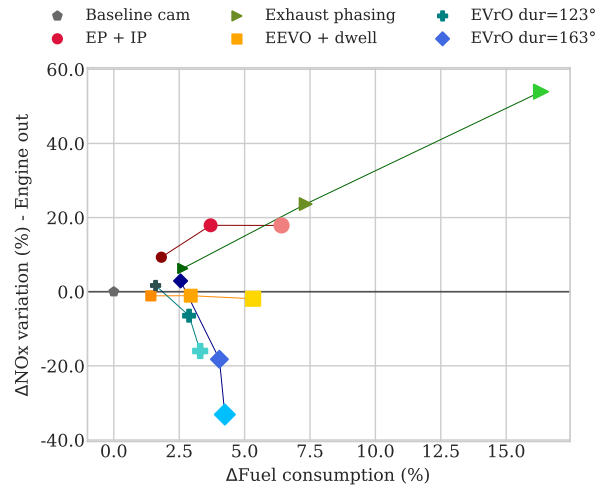


**Figure 13.** Fuel consumption variation (%) against NO<sub>x</sub> engine out variation (%) comparison for all the VVT strategies, taking the baseline case as the reference.

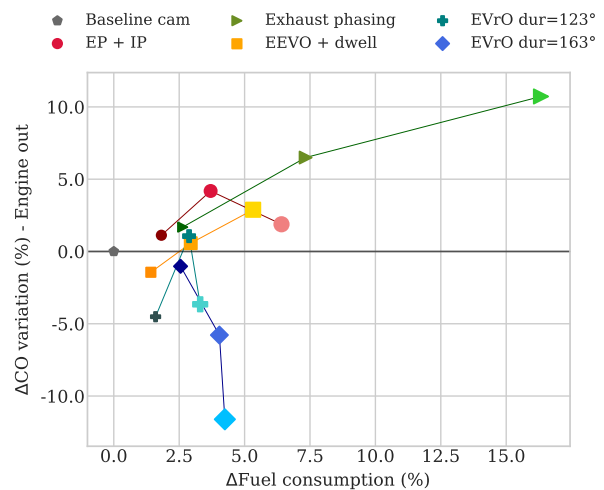


**Figure 14.** Fuel consumption variation (%) against CO engine out variation (%) comparison for all the VVT strategies, taking the baseline case as the reference.

Regarding the trade-off between exhaust temperature and emissions, Figure 15 and Figure 16 present NO<sub>x</sub> and CO trade-offs, respectively. Both figures are similar as the trade-off between fuel consumption and emissions, since the fuel consumption is almost directly proportional to the exhaust temperature in those strategies involving EEVO (“Exhaust

phasing”, “EEVO + dwell”, “EP + IP”). The difference is observed in EVrO strategies. As it can be inferred from Figure 15 and Figure 16, as the increment in exhaust temperature tends to zero,  $\text{NO}_x$  and CO formation are reduced, even reaching levels lower than in the baseline case. This trend can be observed in the trade-off between fuel and emissions as well (Figure 13). The reason is that, as greater the maximum lift of the second exhaust valve event, the greater the IGR, reducing  $\text{NO}_x$  emissions. However, during the transient accelerations, this higher amount of retained residual gases results in lower fresh air charge, leading to a limitation in the injected fuel to avoid excessive soot.

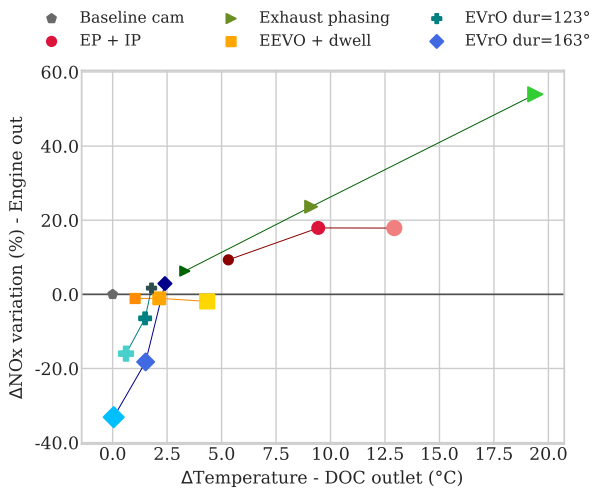


**Figure 15.** DOC outlet temperature variation ( $^{\circ}\text{C}$ ) against  $\text{NO}_x$  engine out variation (%) comparison for all the VVT strategies, taking the baseline case as the reference.

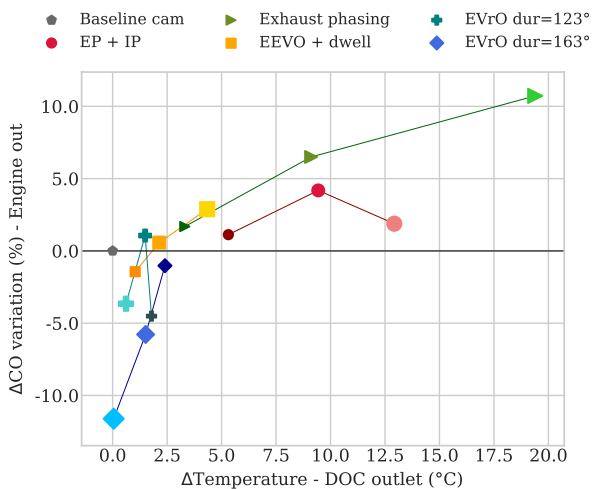


**Figure 16.** DOC outlet temperature variation ( $^{\circ}\text{C}$ ) against CO engine out variation (%) comparison for all the VVT strategies, taking the baseline case as the reference.

## Summary and conclusions

Several variable valve timing strategies were discussed in this paper with the aim of achieve an increment in the exhaust temperature. Several configurations for each strategy were also compared in terms of exhaust temperature profit, fuel

consumption, warm-up time and pollutant emissions. A one-dimensional engine model has been developed and exploited to simulate different VVT strategies at steady and transient (by simulating the entire WLTC) conditions of speed and load. In the spirit to summarize the conclusions obtained along this study, the following points are exposed:

1. Advancing EVO results in an increment in the exhaust temperature due to the early blowdown of hot gases into the exhaust manifold. Advancing also EVC and performing a second exhaust valve event allows a higher exhaust temperature by retaining an amount of the exhaust gases to participate in the next engine cycle (IGR).
2. In the case of EVrO, a long re-opening duration performs better than a longer one in order to increase the exhaust temperature and reduce  $\text{NO}_x$  and CO emissions.
3. “EEVO + dwell” strategy does not produce a relevant increase in exhaust temperature, nor a faster DOC light-off, nor an improvement in pollutant emissions.
4. While, “Exhaust phasing” and “EP + IP” achieve a quicker DOC heat-up, EVrO strategies, on the contrary, increase the time to reach DOC light-off. This is due to the fact that in the transient accelerations where the model is unable to reach the torque target, such as the EVrO with a lift higher than 1mm, the resulting peaks in the temperature downstream the turbine are not reached; thus, the DOC is not heated as quickly as in the baseline case. It could be useful to develop a new calibration when performing EVrO to be able to fulfill torque demand.
5. All VVT strategies incur in a penalty in fuel economy, which is lower for EVrO cases.
6. “EP + IP” strategy presents the best trade-off between exhaust temperature increment and fuel consumption. It also present the best light-off and fuel consumption trade-off. “Exhaust phasing” allows higher exhaust temperature and a faster light-off, but the fuel penalty is far greater.
7. Exhaust valve re-opening presents the best trade-off between  $\text{NO}_x$  and CO emissions and fuel efficiency, being able to reduce both  $\text{NO}_x$  and CO emissions compared to the baseline case. Regarding the other VVT strategies, “EP + IP” presents a better trade-off than “EEVO + dwell” and “Exhaust phasing” strategy, although they increase pollutant emissions levels.

An exhaust advance and an intake delay has been found to be a good technique to reduce DOC heat-up time, increase exhaust temperature and reduce warm-up time. EVrO has been found as a interesting technique in terms of IGR production, exhaust temperature increment, fuel consumption compromise and pollutant emissions reduction, future researches will be focused on extending the use of EVrO strategy in other points of the engine map. However, a proper calibration to extend re-opening operating range and a re-opening phase and lift study have to be carried on.

## Acknowledgements

This research has been partially funded by the European Union’s Horizon 2020 Framework Programme for research, technological



development and demonstration under grant agreement 723976 (“DiePeR”) and by the Spanish government under the grant agreement TRA2017-89894-R. The authors want to acknowledge the “Apoyo para la investigación y Desarrollo (PAID)”, grant for doctoral studies (FPI S2 2018 1048), of Universitat Politècnica de València. The authors also wish to thank Renault SAS, specially P. Mallet for supporting this research.

## References

- Lancefield T, Methley I, Råse U et al. The Application of Variable Event Valve Timing to a Modern Diesel Engine. In *SAE 2000 World Congress*. SAE International. DOI:10.4271/2000-01-1229.
- Gonzalez D M and Di Nunno D. Internal Exhaust Gas Recirculation for Efficiency and Emissions in a 4-Cylinder Diesel Engine. In *SAE 2016 International Powertrains, Fuels and Lubricants Meeting*. SAE International. DOI:10.4271/2016-01-2184.
- Serrano J, Piqueras P, Navarro R et al. Modelling Analysis of Aftertreatment Inlet Temperature Dependence on Exhaust Valve and Ports Design Parameters. In *SAE 2016 World Congress and Exhibition*. SAE International. DOI:10.4271/2016-01-0670.
- Siewert R. How Individual Valve Timing Events Affect Exhaust Emissions. In *International Mid-Year Meeting*. 710609, SAE International. DOI:10.4271/710609.
- Tomoda T, Ogawa T, Ohki H et al. Improvement of Diesel Engine Performance by Variable Valve Train System. *International Journal of Engine Research* 2010; 11(5): 331–344. DOI:10.1243/14680874JER586.
- Benajes J, Reyes E and Luján JM. Modelling Study of the Scavenging Process in a Turbocharged Diesel Engine with Modified Valve Operation. *Proceedings of the Institution of Mechanical Engineers, Part C: Journal of Mechanical Engineering Science* 1996; 210(4): 383–393. DOI:10.1243/PIME.PROC.1996.210.210.02.
- Deppenkemper K, Özyalcin C, Ehrly M et al. 1D Engine Simulation Approach for Optimizing Engine and Exhaust Aftertreatment Thermal Management for Passenger Car Diesel Engines by Means of Variable Valve Train (VVT) Applications. In *WCX World Congress Experience*. SAE International. DOI:10.4271/2018-01-0163.
- Zammit J, McGhee M, Shayler P et al. The effects of early inlet valve closing and cylinder disablement on fuel economy and emissions of a direct injection diesel engine. *Energy* 2015; 79: 100 – 110. DOI:10.1016/j.energy.2014.10.065.
- Piano A. *Analysis of Advanced Air and Fuel Management Systems for Future Automotive Diesel Engine Generation*. PhD Thesis, Politecnico di Torino, 2018.
- Guan W, Pedrozo VB, Zhao H et al. Variable valve actuation–based combustion control strategies for efficiency improvement and emissions control in a heavy-duty diesel engine. *International Journal of Engine Research* 2019; DOI: 10.1177/1468087419846031.
- Guan W, Zhao H, Ban Z et al. Exploring alternative combustion control strategies for low-load exhaust gas temperature management of a heavy-duty diesel engine. *International Journal of Engine Research* 2019; 20(4): 381–392. DOI: 10.1177/1468087418755586.
- Maniatis P, Wagner U and Koch T. A model-based and experimental approach for the determination of suitable variable valve timings for cold start in partial load operation of a passenger car single-cylinder diesel engine. *International Journal of Engine Research* 2019; 20(1): 141 – 154. DOI: 10.1177/1468087418817119.
- Kim J and Choongsik B. An investigation on the effects of late intake valve closing and exhaust gas recirculation in a single-cylinder research diesel engine in the low-load condition. *Proceedings of the Institution of Mechanical Engineers, Part D: Journal of Automobile Engineering* 2016; 230(6): 771–787. DOI:10.1177/0954407015595149.
- Zhou X, Liu E, Sun D et al. Study on transient emission spikes reduction of a heavy-duty diesel engine equipped with a variable intake valve closing timing mechanism and a two-stage turbocharger. *International Journal of Engine Research* 2019; 20(3): 277–291. DOI:10.1177/1468087417748837.
- Gosala DB, Ramesh AK, Allen CM et al. Diesel engine aftertreatment warm-up through early exhaust valve opening and internal exhaust gas recirculation during idle operation. *International Journal of Engine Research* 2018; 19(7): 758–773. DOI:10.1177/1468087417730240.
- Parvate-Patil G, Hong H and Gordon B. Analysis of Variable Valve Timing Events and Their Effects on Single Cylinder Diesel Engine. In *2004 Powertrain and Fluid Systems Conference and Exhibition*. SAE International. DOI:10.4271/2004-01-2965.
- Piano A and Millo F. Numerical Analysis on the Potential of Different Variable Valve Actuation Strategies on a Light Duty Diesel Engine for Improving Exhaust System Warm Up. In *13th International Conference on Engines and Vehicles*. SAE International. DOI:10.4271/2017-24-0024.
- Martín J, Arnau F, Piqueras P et al. Development of an Integrated Virtual Engine Model to Simulate New Standard Testing Cycles. In *WCX World Congress Experience*. SAE International. DOI:10.4271/2018-01-1413.
- Serrano JR, Arnau F, García-Cuevas L et al. Development and validation of a radial turbine efficiency and mass flow model at design and off-design conditions. *Energy Conversion and Management* 2016; 128: 281–293. DOI:10.1016/j.enconman.2016.09.032.
- Serrano JR, Olmeda P, Arnau F et al. A holistic methodology to correct heat transfer and bearing friction losses from hot turbocharger maps in order to obtain adiabatic efficiency of the turbomachinery. *International Journal of Engine Research* in press; DOI:10.1177/1468087419834194.
- Arrègle J, López JJ, Martín J et al. Development of a Mixing and Combustion Zero-Dimensional Model for Diesel Engines. In *SAE 2006 World Congress and Exhibition*. SAE International. DOI:10.4271/2006-01-1382.
- Payri F, Arrègle J, López JJ et al. Diesel NOx Modeling with a Reduction Mechanism for the Initial NOx Coming from EGR or Re-entrained Burned Gases. In *SAE World Congress and Exhibition*. SAE International. DOI:10.4271/2008-01-1188.
- Broatch A, Olmeda P, Martín J et al. Development and Validation of a Submodel for Thermal Exchanges in the Hydraulic Circuits of a Global Engine Model. In *WCX World Congress Experience*. SAE International. DOI:10.4271/2018-01-0160.
- Russell A and Epling W. Diesel Oxidation Catalysts. *Catalysis Reviews* 2011; 53(4): 337–423. DOI:10.1080/01614940.2011.

- 596429.
25. Payri F, Arnau F, Piqueras P et al. Lumped Approach for Flow-Through and Wall-Flow Monolithic Reactors Modelling for Real-Time Automotive Applications. In *WCX World Congress Experience*. SAE International. DOI:10.4271/2018-01-0954.
  26. Guardiola C, Pla B, Piqueras P et al. Model-based passive and active diagnostics strategies for diesel oxidation catalysts. *Applied Thermal Engineering* 2017; 110: 962 – 971. DOI: 10.1016/j.applthermaleng.2016.08.207.
  27. Abdelghaffar WA, Osman MM, Saeed MN et al. Effects of Coolant Temperature on the Performance and Emissions of a Diesel Engine. In *ASME 2002 Internal Combustion Engine Division Spring Technical Conference*. ICES2002-464, pp. 187–197. DOI:10.1115/ICES2002-464.
  28. Torregrosa A, Olmeda P, Martín J et al. Experiments on the influence of inlet charge and coolant temperature on performance and emissions of a DI Diesel engine. *Experimental Thermal and Fluid Science* 2006; 30(7): 633 – 641. DOI:10.1016/j.exptthermflusci.2006.01.002.
  29. Guardiola C, Pla B, Bares P et al. An on-board method to estimate the light-off temperature of diesel oxidation catalysts. *International Journal of Engine Research* 2018; DOI:10.1177/1468087418817965.

## Nomenclature

### List of abbreviations

<b>0D</b>	Zero-dimensional
<b>1D</b>	One-dimensional
<b>BDC</b>	Bottom Dead Centre
<b>BMEP</b>	Brake Mean Effective Pressure
<b>BSFC</b>	Brake Specific Fuel Consumption
<b>CI</b>	Compression Ignited
<b>CO</b>	Carbon monoxide
<b>DOC</b>	Diesel Oxidation Catalyst
<b>DPF</b>	Diesel Particle Filter
<b>EAT</b>	Exhaust After-Treatment
<b>ECU</b>	Engine Control Unit
<b>EEVC</b>	Early Exhaust Valve Closing
<b>EEVO</b>	Early Exhaust Valve Opening
<b>EGR</b>	Exhaust Gas Recirculation
<b>EIVC</b>	Early Intake Valve Closing
<b>EIVO</b>	Early Intake Valve Opening
<b>EVC</b>	Exhaust Valve Closing
<b>EVO</b>	Exhaust Valve Opening
<b>EVRO</b>	Exhaust Valve re-Opening
<b>HC</b>	Hydrocarbons
<b>HP-EGR</b>	High Pressure EGR
<b>HSDI</b>	High Speed Direct Injection
<b>IGR</b>	Internal Gas Recirculation
<b>IVC</b>	Intake Valve Closing
<b>IVO</b>	Intake Valve Opening
<b>LEVC</b>	Late Exhaust Valve Closing
<b>LEVO</b>	Late Exhaust Valve Opening
<b>LIVC</b>	Late Intake Valve Closing
<b>LIVO</b>	Late Intake Valve Opening
<b>LP-EGR</b>	Low Pressure EGR
<b>NO<sub>x</sub></b>	Nitrogen oxides
<b>SI</b>	Spark Ignited
<b>SOI</b>	Start of injection
<b>TDC</b>	Top Dead Centre
<b>VEMOD</b>	Virtual Engine Model
<b>VGT</b>	Variable Geometry Turbine
<b>VVA</b>	Variable Valve Actuation
<b>VVT</b>	Variable Valve Timing
<b>WLTC</b>	Worldwide Harmonized Light-Duty Vehicles Test Cycle

### List of symbols

$\lambda$	Air-fuel equivalence ratio
-----------	----------------------------